**Supplementary materials**

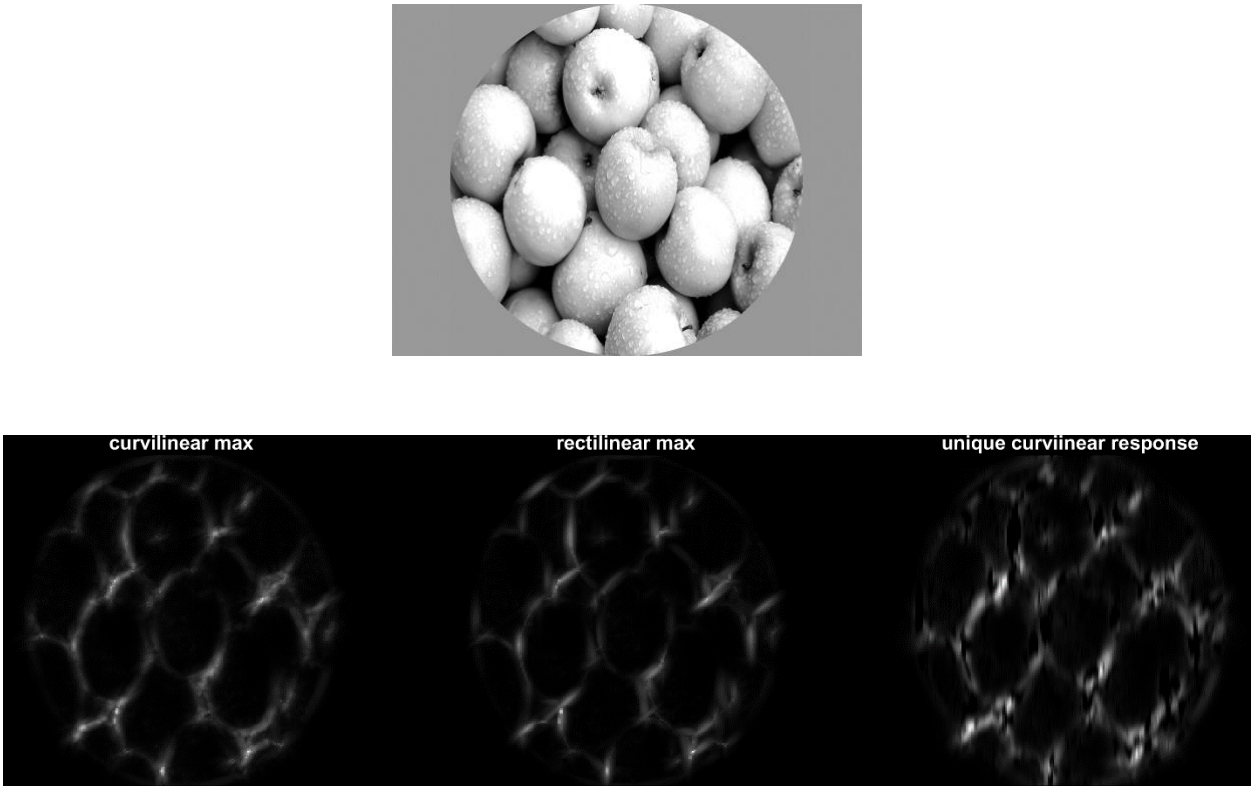


Figure S1. Illustration of image curvature quantification. An example of an image used in the experiment is shown on the top. After preprocessing, the image was convolved with the bank of curved Gabor filters to create 120 (3 x 8 x 5) curved Gabor coefficient images. Then, the largest magnitude across all 120 curved Gabor coefficient images was extracted for each pixel to create a peak curved Gabor coefficient image shown on the bottom left. The same procedure was repeated using the bank of rectilinear Gabor filters to generate a peak rectilinear Gabor coefficient image shown in bottom middle. Next, the magnitude in the peak curved Gabor coefficient image was set to zero at a pixel if its magnitude was smaller than that in the peak rectilinear Gabor coefficient image in that pixel. The procedure went through all pixels to create a curved Gabor coefficient image with no rectilinear features represented, which we called a unique curved Gabor coefficient image and is shown on the bottom right. Finally, a curvilinear value of the stimulus image was produced by averaging the unique curved Gabor coefficient image across all pixels. All three images on the bottom are shown in the same scale.

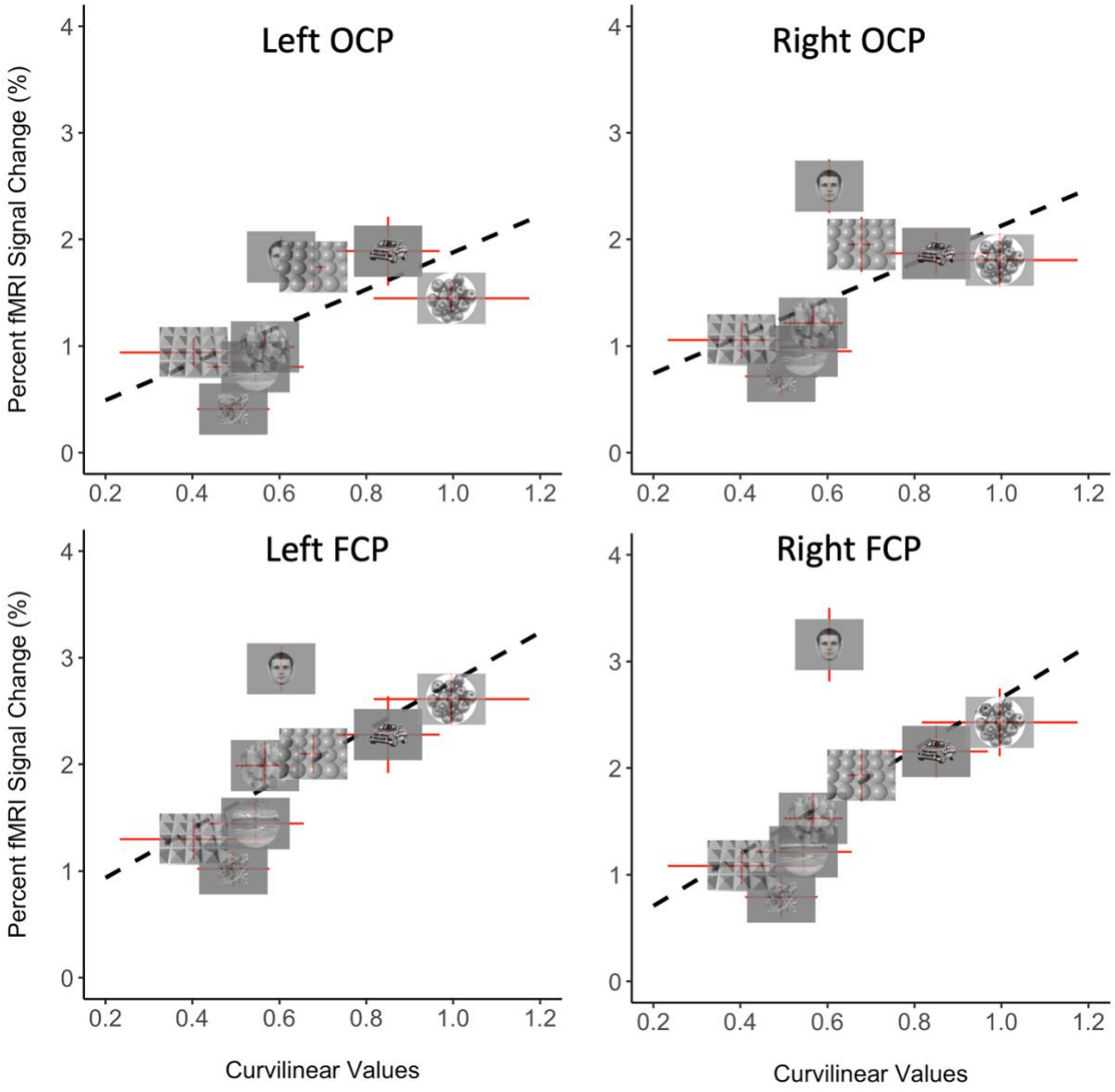


Figure S2. Correlations of fMRI activity with curvilinear values in curvature-preferring patches were not significant in left OCP (r = 0.579, $p$ = 0.132), right OCP (r =0.495, $p$ = 0.212), left FCP (r =0.642, $p$ = 0.086), or right FCP (r = 0.554, $p$ = 0.155). Eight images were presented in each condition. A single curvilinear value was assigned to a condition by averaging the eight curvilinear values of all images in that condition. In a condition, a single value of percent signal change was calculated by averaging across subjects' responses in an ROI defined in the subject's native space. All error bars represent the S.E.M. Non-significant correlations observed for these curvature-selective patches suggest that they are not involved in processing simple curvilinear features, such as curved lines that could be modelled and quantified by curved-Gabor filters (see Methods).

Left OCP

| Intercept | Low-Curvature | Mid-Curvature | High-Curvature | predicted condition |
|---|---|---|---|---|
| 0.783 | -38.341 | 9.954 | 51.297 | faces |
| 0.987 | -51.709 | 70.149 | 33.168 | objects |
| 1.064 | -50.183 | 77.812 | 25.441 | scramble |
| 0.922 | -45.766 | 71.385 | 27.188 | scenes |
| 1.206 | -57.021 | 91.604 | 22.383 | curvilinear shapes |
| 1.003 | -53.959 | 85.687 | 26.657 | rectilinear shape |
| 1.117 | -57.959 | 79.331 | 33.403 | spheres |
| 1.01 | -51.031 | 70.529 | 31.292 | pyramids |

Right OCP

| Intercept | Low-Curvature | Mid-Curvature | High-Curvature | predicted condition |
|---|---|---|---|---|
| 0.985 | -40.814 | 24.041 | 47.067 | faces |
| 1.403 | -67.094 | 144.579 | 9.766 | objects |
| 1.627 | -63.252 | 168.836 | -12.411 | scramble |
| 1.296 | -57.745 | 146.41 | 0.562 | scenes |
| 1.705 | -74.349 | 174.135 | -5.206 | curvilinear shapes |
| 1.424 | -71.893 | 174.737 | -1.971 | rectilinear shapes |
| 1.679 | -81.701 | 164.489 | 11.977 | spheres |
| 1.4 | -66.031 | 149.993 | 5.101 | pyramids |

Table 1. Low, medium, and high curvature weights calculated from the linear combination analyses (see Methods) for left (top) and right (bottom) OCP.

Left FCP

| Intercept | Low-Curvature | Mid-Curvature | High-Curvature | predicted condition |
|---|---|---|---|---|
| 0.469 | -3 | -99.017 | 87.509 | faces |
| 1.066 | -38.36 | 67.807 | 33.824 | objects |
| 1.235 | -35.562 | 86.427 | 17.149 | scramble |
| 0.833 | -22.337 | 69.521 | 20.628 | scenes |
| 1.453 | -48.941 | 106.794 | 15.88 | curvilinear shapes |
| 1.069 | -48.167 | 120.301 | 16.421 | rectilinear shapes |
| 1.452 | -61.036 | 96.294 | 39.854 | spheres |
| 1.18 | -38.001 | 55.474 | 37.325 | pyramids |

Right FCP

| Intercept | Low-Curvature | Mid-Curvature | High-Curvature | predicted condition |
|---|---|---|---|---|
| 0.411 | -15.001 | -59.112 | 76.268 | faces |
| 1.195 | -64.229 | 166.827 | 6.284 | objects |
| 1.689 | -55.971 | 220.977 | -42.487 | scramble |
| 1.033 | -49.174 | 170.076 | -9.081 | scenes |
| 1.707 | -76.274 | 216.79 | -19.413 | curvilinear shapes |
| 1.235 | -71.8 | 216.108 | -13.456 | rectilinear shapes |
| 1.726 | -92.609 | 205.276 | 10.834 | spheres |
| 1.091 | -62.042 | 189.95 | -7.613 | pyramids |

Table 2. Low, medium, and high curvature weights calculated from the linear combination analyses (see Methods) for left (top) and right (bottom) FCP.

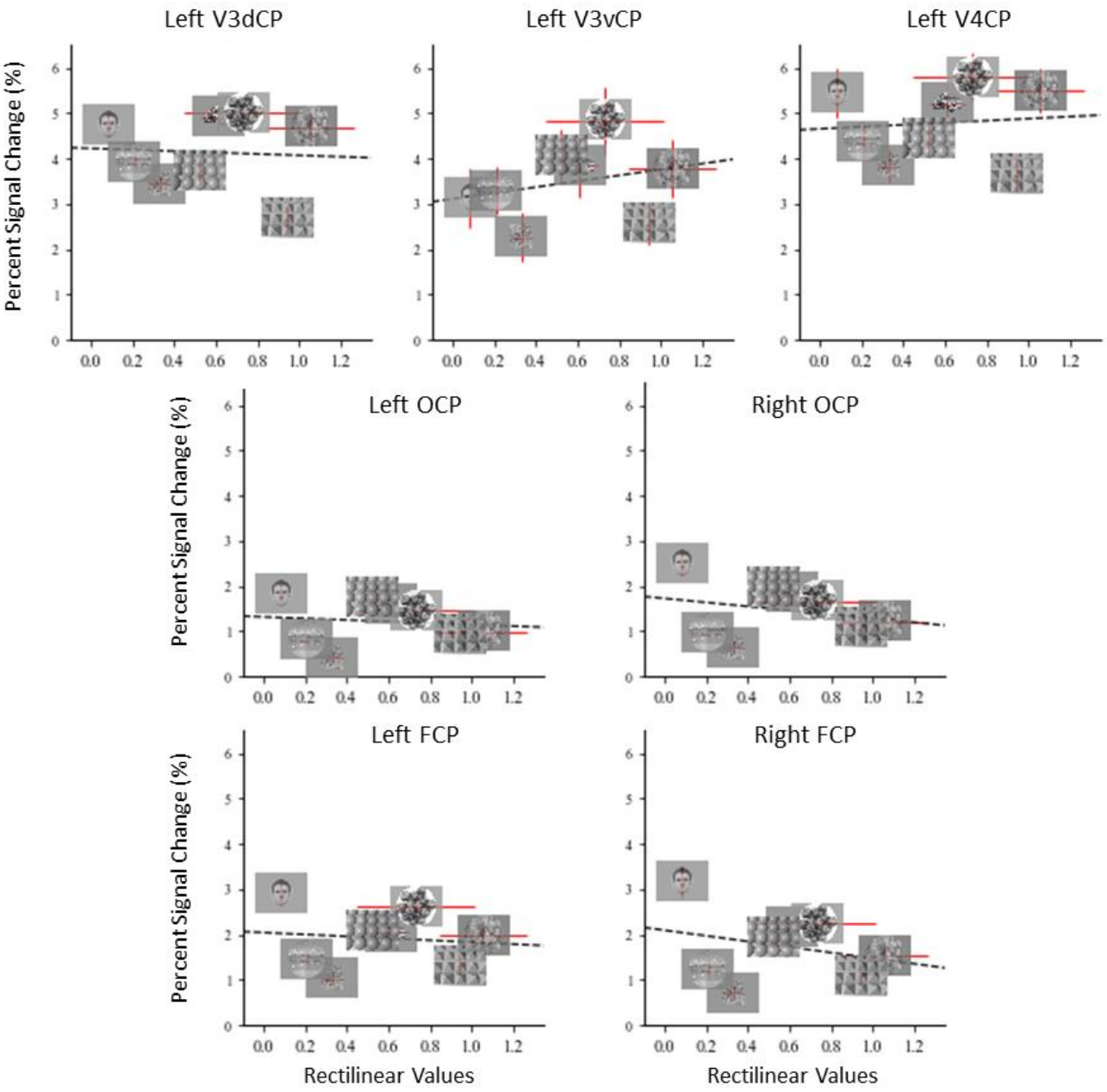


Figure S3. Correlation of rectilinear values of visual stimuli and fMRI response in curvature-preferring patches. Correlations were not significant in left V3dCP (r = -0.063, $p$ = 0.882), left V3vCP (r = 0.095, $p$ = 0.823), left V4CP (r = 0.266, $p$ = 0.524), left OCP (r = -0.115, $p$ = 0.787), right OCP (r = -0.246, $p$ = 0.558), left FCP (r = -0.114, $p$ = 0.789), or right FCP (r = -0.271, $p$ = 0.516).

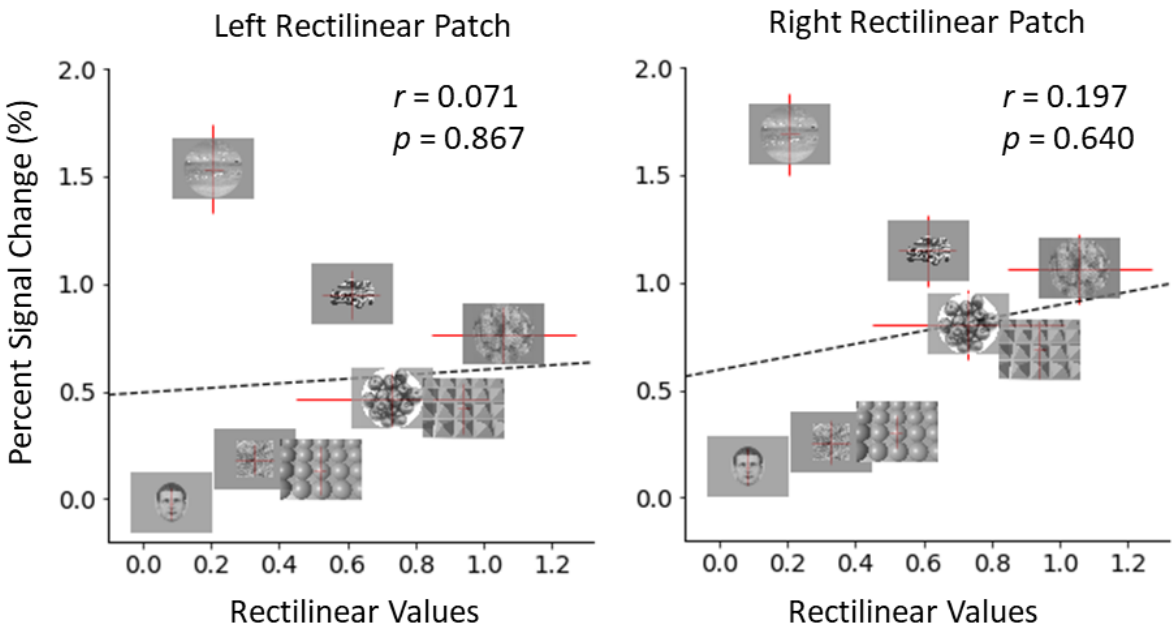


Figure S4. Correlation between rectilinear values of visual stimuli and fMRI response in the bilateral rectilinear preferring patches. No significant correlation was found in either hemisphere (left: r = 0.071, *p* = 0.867; right: r = 0.197, *p* = 0.640).

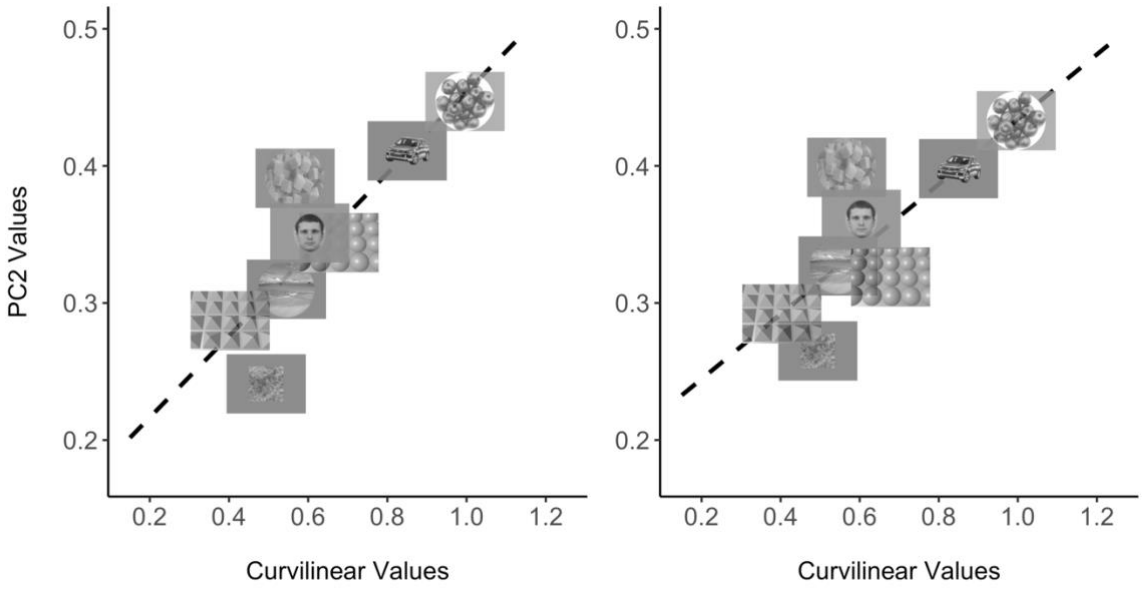


Figure S5. Correlation of the PC2 loadings with curvilinear values for left (left) and right (right) hemisphere responses at the group level. Significant correlations for left (r = 0.851, $p$ = 0.007) and right hemisphere (r = 0.791, $p$ = 0.0195) indicate that the PC2 is relevant to curvilinearity of visual stimuli.

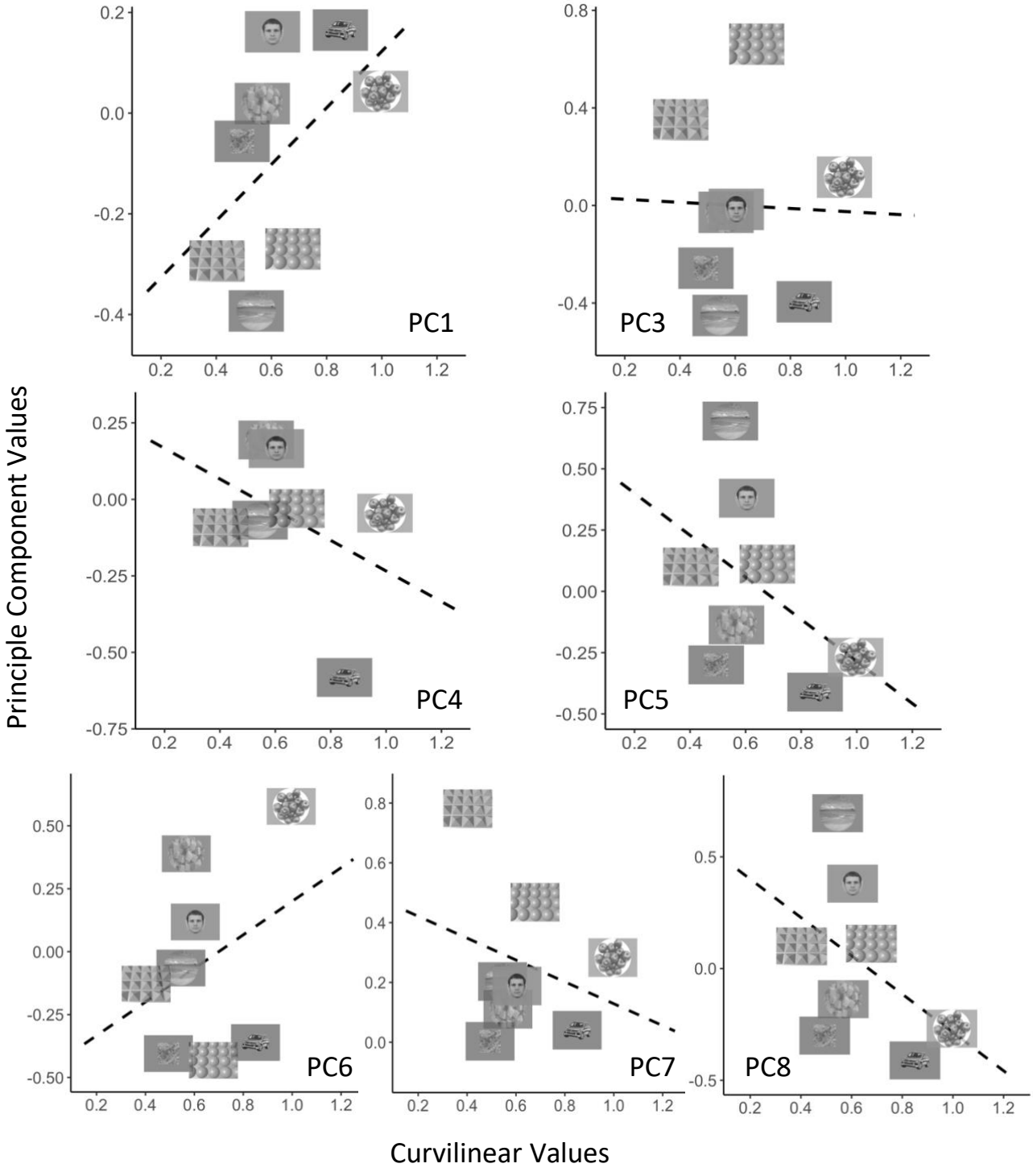


Figure S6. Correlation of PC1, PC3, PC4, PC5, PC6, PC7, and PC8 with curvilinear values for the left hemisphere at the group level. None of the correlations were significant: PC1 (r = 0.508, $p$ = 0.198), PC3 ( r = -0.032, $p$ = 0.939), PC4 (r = -0.474, $p$ = 0.235), PC5 ( r = -0.443, $p$ = 0.272), PC6 (r = 0.346, $p$ = 0.401), PC7 (r = -0.278, $p$ = 0.505), PC8 (r = -0.443, $p$ = 0.272).

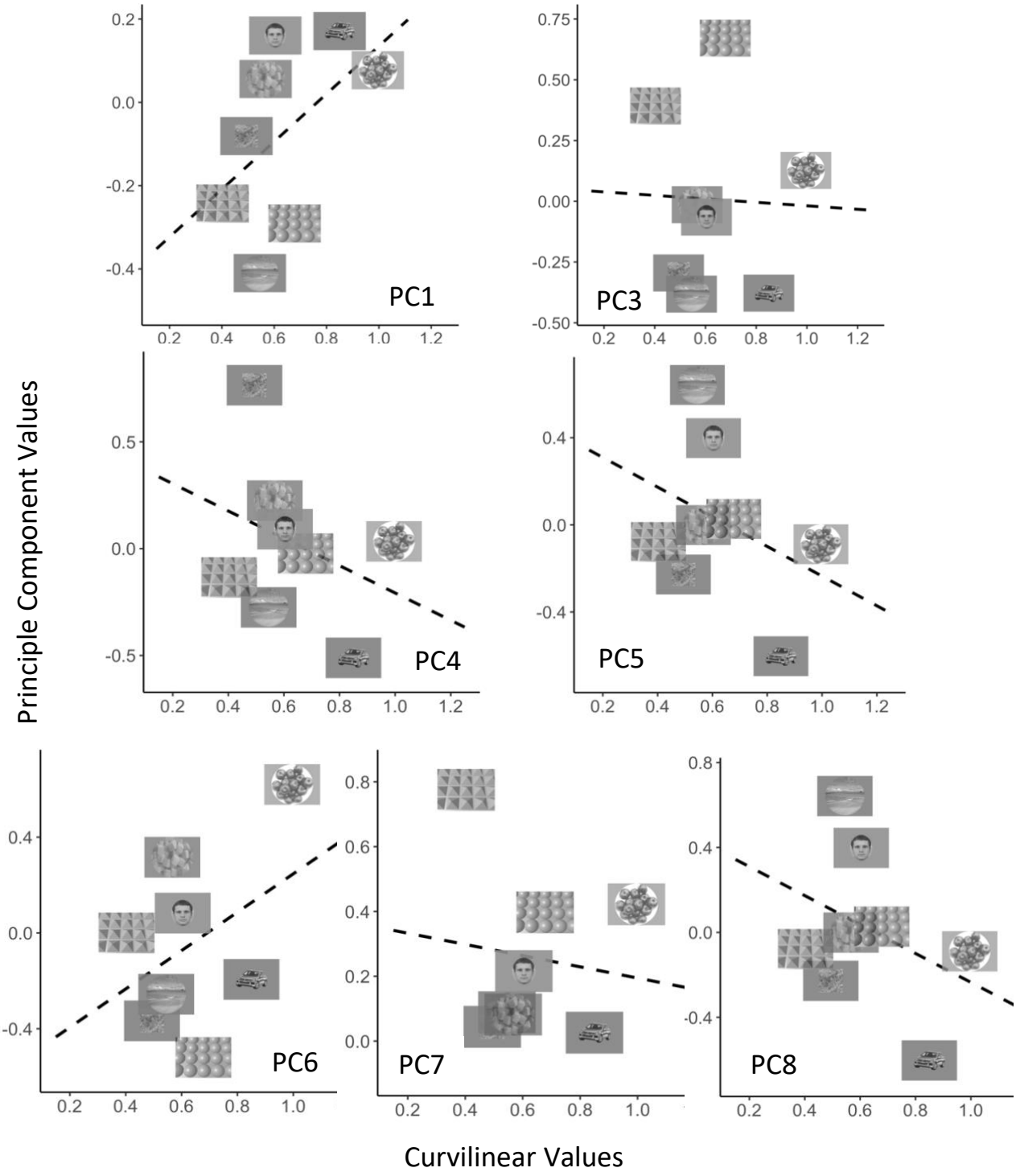


Figure S7. Correlation of PC1, PC3, PC4, PC5, PC6, PC7, and PC8 with curvilinear values for the right hemisphere at the group level. None of the correlations were significant: PC1 (r = 0.504, $p$ = 0.203), PC3 ( r = - 0.037, $p$ = 0.931), PC4 (r = -0.330, $p$ = 0.425), PC5 ( r = -0.351, $p$ = 0.394), PC6 (r = 0.416, $p$ = 0.306), PC7 (r = -0.129, $p$ = 0.760), PC8 (r = -0.351, $p$ = 0.394).

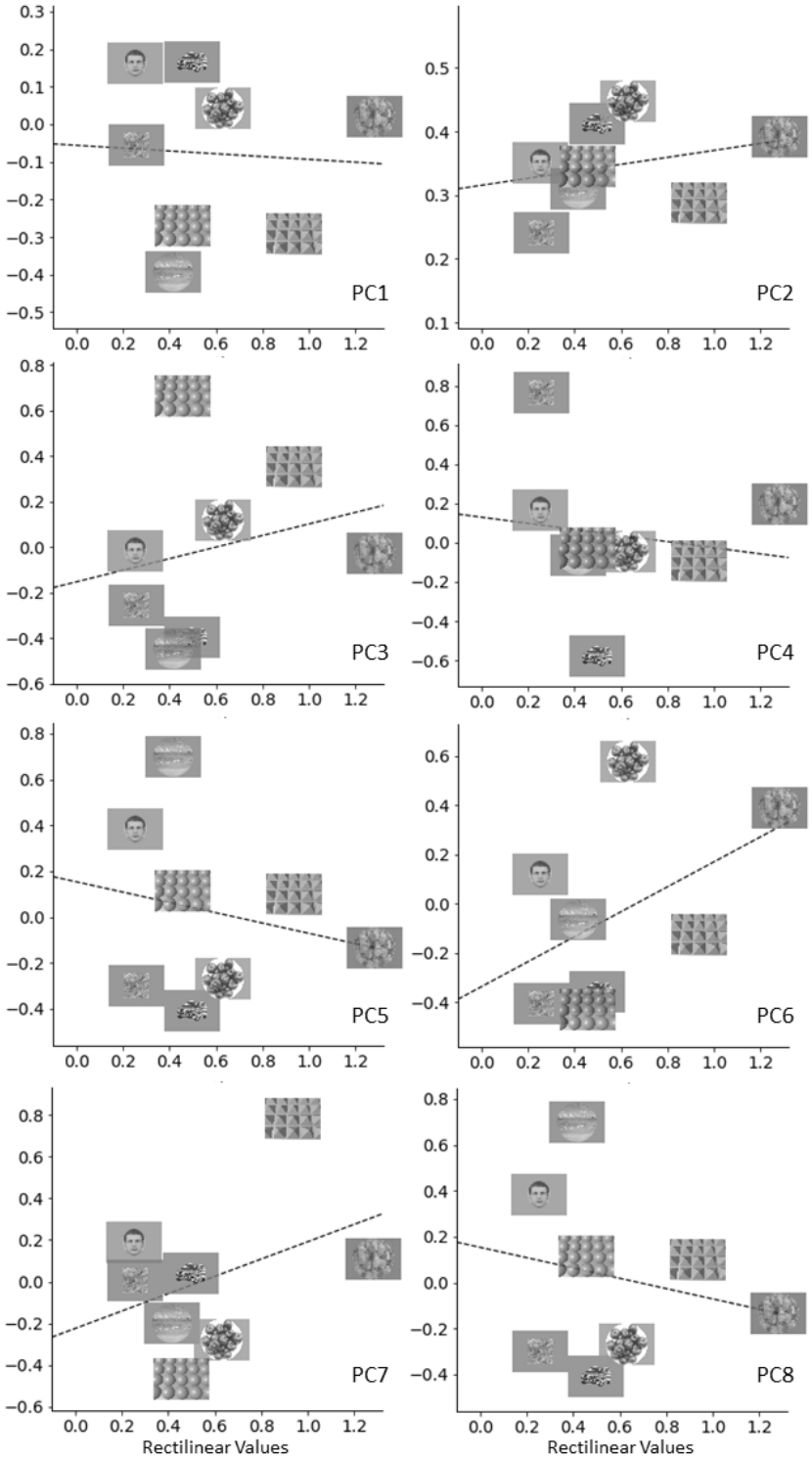


Figure S8. Correlation of PC1, PC2, PC3, PC4, PC5, PC6, PC7, and PC8 with rectilinear values for the left hemisphere at the group level. None of the correlations were significant: PC1 (r = -0.062, $p$ = 0.885), PC2 (r = 0.286, $p$ = 0.493), PC3 (r = 0.239, $p$ = 0.569), PC4 (r = -0.147, $p$ = 0.728), PC5 (r = -0.211, $p$ = 0.616), PC6 (r = 0.478, $p$ = 0.231), PC7 (r = 0.391, $p$ = 0.338), PC8 (r = -0.211, $p$ = 0.616).

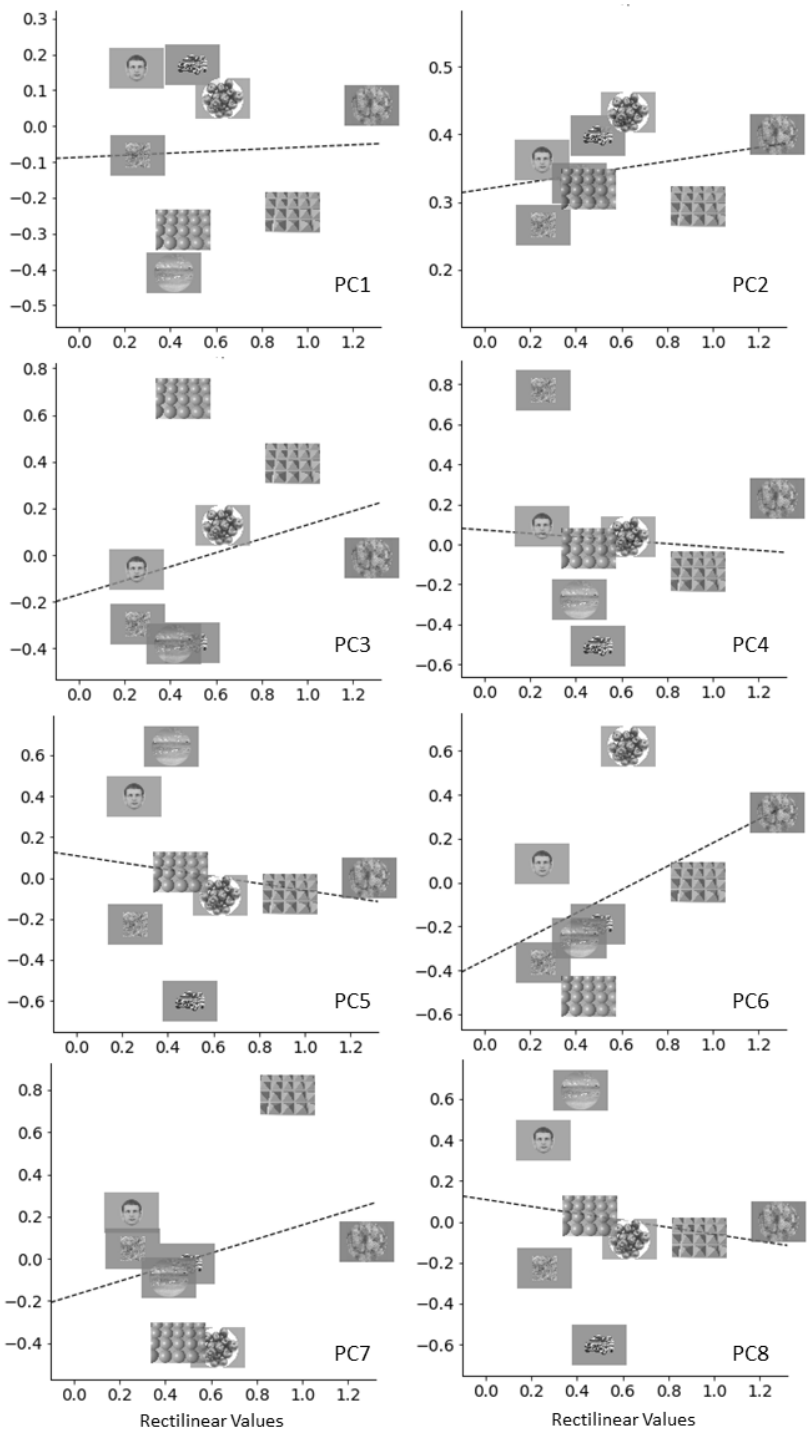


Figure S9. Correlation of PC1, PC2, PC3, PC4, PC5, PC6, PC7, and PC8 with rectilinear values for the right hemisphere at the group level. None of the correlations were significant: PC1 (r = 0.047, $p$ = 0.913), PC2 (r = 0.312, $p$ = 0.451), PC3 (r = 0.279, $p$ = 0.563), PC4 (r = -0.079, $p$ = 0.852), PC5 (r = -0.159, $p$ = 0.707), PC6 (r = 0.505, $p$ = 0.202), PC7 (r = 0.313, $p$ = 0.451) , PC8 (r = -0.159, $p$ = 0.707).

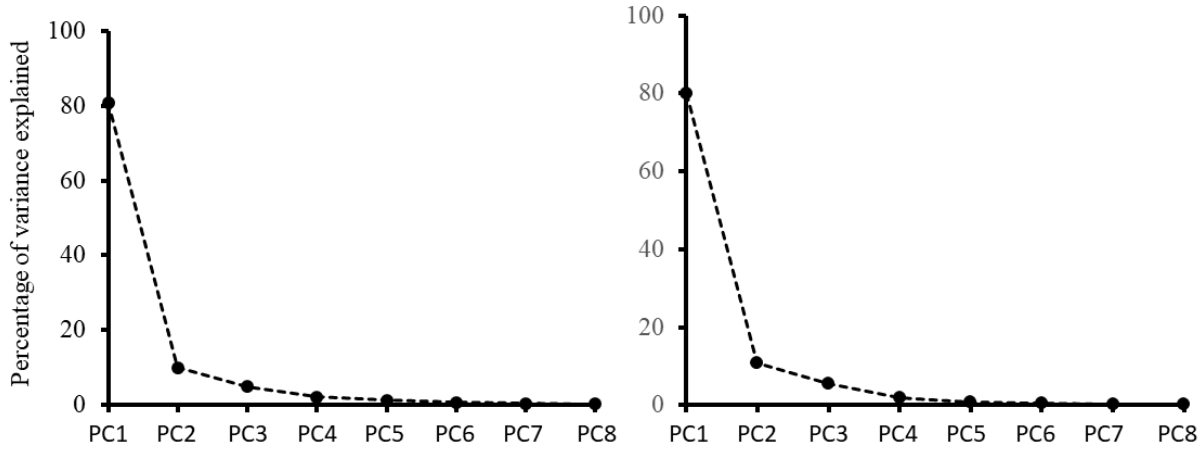


Figure S10. The percentage of variance explained by each principle component (PC) for left (left) and right (right) hemispheres calculated using group data.

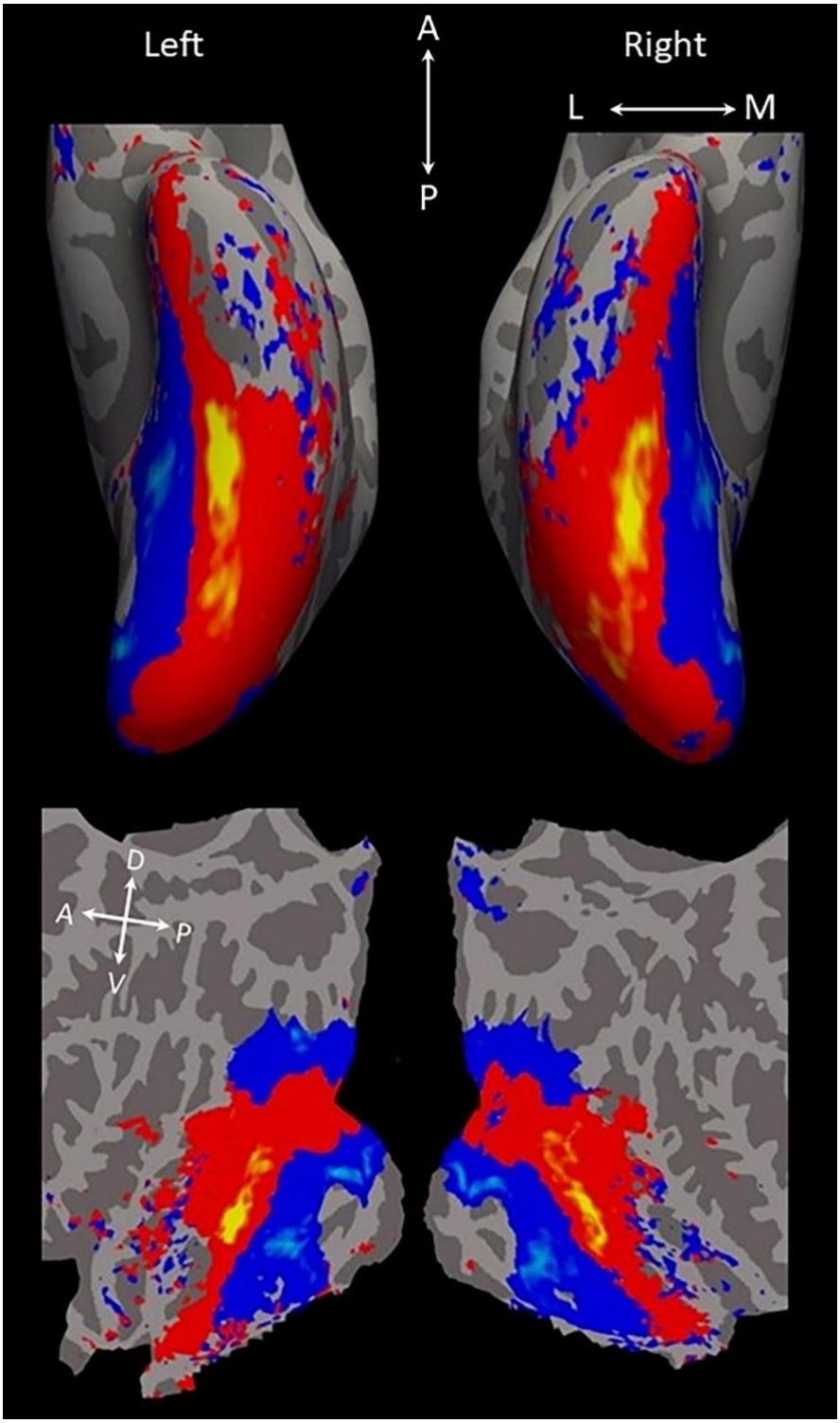


Figure S11. Group PCA map generated without data from the face condition. This PC2 map is similar to the PC2 map generated with data from all conditions (Figure 8), which suggests that the PC2 map generated from this experiment is not dominated by the face condition. Local orientation of the brain axes on the flattened brain are indicated in white letter (D = dorsal; V = ventral; P = posterior; A = anterior).

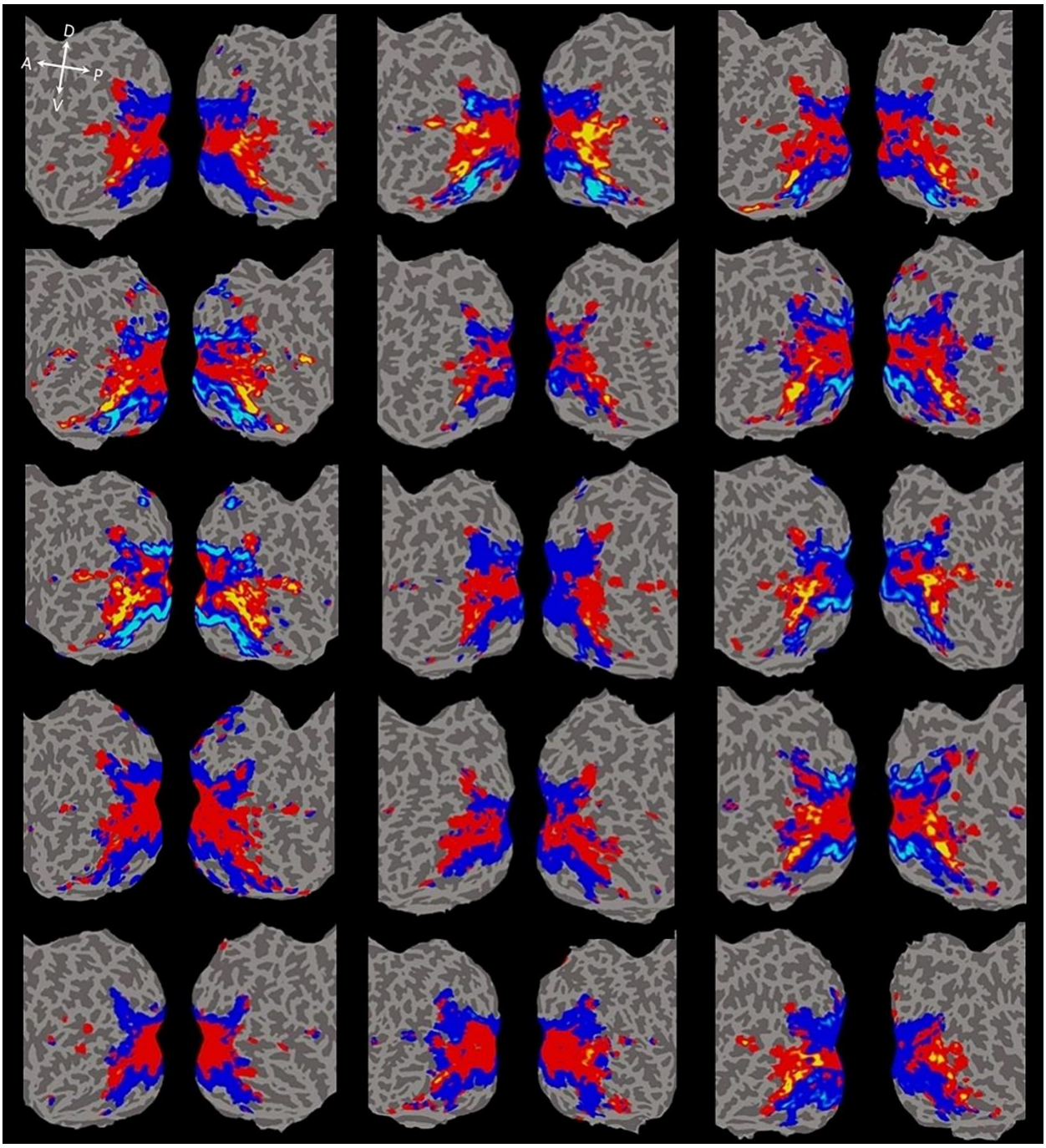


Figure S12. Individual subject PCA maps generated without data from the face condition. Each subject's data were projected onto their native flattened surface. We observed similar PC2 maps for each subject as the PCA maps in Figure 9 generated with the face condition. Local orientation of the brain axes on the flattened brain are indicated in white letter (D = dorsal; V = ventral; P = posterior; A = anterior).